JACS
JOURNAL OF THE AMERICAN CHEMICAL SOCIETY
pubs.acs.org/JACS
Communication

Onium Photocages for Visible-Light-Activated Poly(thiourethane) Synthesis and 3D Printing

Meghan T. Kiker,‡ Ain Uddin,‡ Lynn M. Stevens, Connor J. O'Dea, Keldy S. Mason, and Zachariah A. Page*

Cite This: J. Am. Chem. Soc. 2024, 146, 19704−19709
Read Online
ACCESS | Metrics & More | Article Recommendations | Supporting Information

ABSTRACT: The lack of chemical diversity in light-driven reactions for 3D printing poses challenges in the production of structures with long-term ambient stability, recyclability, and breadth in properties (mechanical, optical, etc.). Herein we expand the scope of photochemistries compatible with 3D printing by introducing onium photocages for the rapid formation of poly(thiourethanes) (PTUs). Efficient nonsensitized visible-light photolysis releases organophosphine and -amine derivatives that catalyze thiol−isocyanate polyaddition reactions with excellent temporal control. Two resin formulations comprising commercial isocyanates and thiols were developed for digital light processing (DLP) 3D printing to showcase the fast production of high-resolution PTU objects with disparate mechanical properties. Onium photocages represent valuable tools to advance light-driven manufacturing of next-generation high-performance sustainable materials.

Light-driven chemistry has enabled numerous technologies, from lithography to produce microelectronics to emergent additive manufacturing in the fabrication of medical devices.[1−5] These transformative discoveries rely on the spatiotemporal control offered by light in polymer synthesis. Light-induced radical polymerizations have dominated over ionic ones because of their lower photoinitiator cost, excellent temporal control, and faster, application-relevant, reaction speeds (completion in <60 s). However, radical-based photopolymerizations are majorly limited in scope to acrylics and, more recently, thiol−ene reactions.[6−9]

Anionic photopolymerizations can diversify the portfolio of accessible polymers to include polysulfides,[10−15] polyesters,[16,17] polyamides,[18,19] and poly((thio)urethanes) (P(T)Us).[20−22] In these polymers, the heteroatomic backbones provide intermolecular interactions that can improve mechanical performance (e.g., strength and toughness) while simultaneously enabling plastic recyclability.[23−26] Among them, polythiourethanes from thiol−isocyanate addition stand-out in reaction speed, exceptional thermomechanical and optical properties (e.g., high toughness, hardness, and refractive index), and ease of triggered dynamic bond exchange for reprocessability.[27−31] However, a lack of temporal control[21] has precluded advanced manufacturing of PTUs.

In parallel with our efforts, Sardon and co-workers demonstrated the first example of PTU digital light processing (DLP) 3D printing via UV-light-driven sensitization of a commercial guanidinium photobase generator.[32] The authors showcased the utility of such networks in both recyclable photoresins and self-healing constructs. However, poor solubility of the ionic photobase in the resin necessitated use of a volatile solvent (30 wt % acetone), which can compromise resin stability, produce secondary waste, and cause part shrinkage. Additionally, the two-component photosystem results in diffusion limitations that can restrict the printable resin viscosity.

Described herein are single-component onium photocages that provide exceptional temporal activation of thiol−isocyanate addition, providing PTUs in a matter of seconds upon light exposure. Moreover, activation by low-intensity visible LEDs is accomplished without sensitization[10,13,14] or uncaging via decarboxylation,[23,24] where CO_2 gas evolution can cause termination from acidification and mechanical embrittlement from voids.

Photocage design was constructed on four pillars: (1) *o*-nitrobenzyl (***o*NB**) for efficient uncaging, (2) tetraphenylborate counteranions[33] to avoid CO_2 gas release, (3) phosphine cargo to rapidly catalyze thiol−isocyanate addition, and (4) onium cages for temporal control (Figure 1A). A range of ***o*NB** photobase generators (PBGs) were synthesized via a scalable three-step process. First, PBr_3 converts 4,5-dimethoxy-2-nitrobenzyl alcohol to the corresponding bromide, followed by nucleophilic substitution with the desired amine or phosphine. Specifically, tributylamine (**TBA**), tripropylphosphine (**TPP**), dimethylphenylphosphine (**DMPP**), and methyldiphenylphosphine (**MDPP**) were selected. Finally, anion exchange of bromide for tetraphenylborate ($[BPh_4]^-$) was conducted in water (see section S1.2 for further details). The overall yield for the three-step synthesis was 60% (**DMPP**), which facilitated gram-scale photocage preparation (Figure 1B, inset). A neutral photocage bearing tetramethylguanidine

Received: May 27, 2024
Revised: July 3, 2024
Accepted: July 5, 2024
Published: July 9, 2024

https://doi.org/10.1021/jacs.4c07220
J. Am. Chem. Soc. 2024, 146, 19704−19709

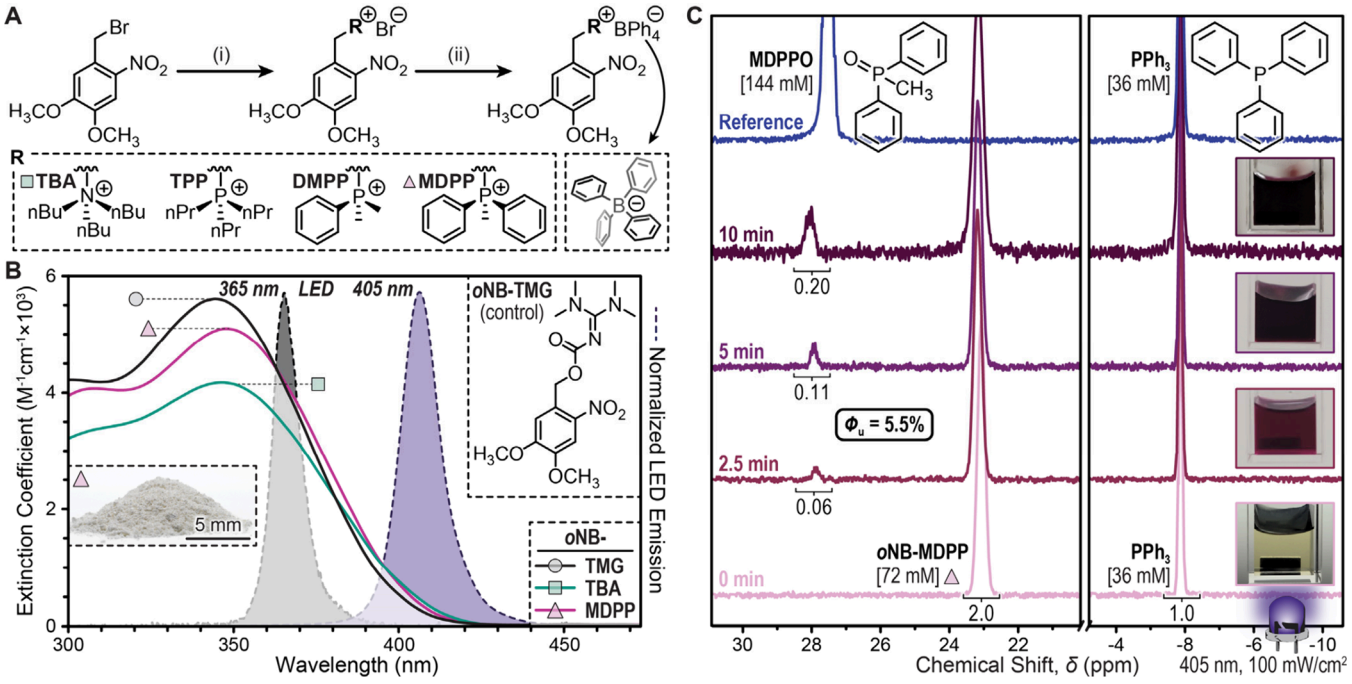

Figure 1. Onium photocage synthesis and characterization. (A) Scalable synthetic protocol to [***o*NB-R**]$^+$[BPh_4]$^-$ photocages. Conditions: (i) base (R = TBA, MDPP, etc.), toluene, rt, 3 h, >98% yield; (ii) 2% aq. HCl, BPh_4, rt, 2 h, >77% yield. (B) Representative photocage UV−vis absorption spectra in CH_3CN (8 mM) underlaid with UV (365 nm) and violet (405 nm) LED profiles. The inset photograph shows the gram-scale yield of ***o*NB-MDPP**. (C) ^{31}P NMR spectra showing the generation of **MDPPO** upon irradiation with violet light to determine the uncaging quantum yield (Φ_u).

(***o*NB-TMG**)[10,34] was also prepared and tested as a control. UV−vis absorption spectroscopy revealed peak absorption bands at ∼350 nm that tailed into the visible (>400 nm) spectrum for all ***o*NB** derivatives (Figures 1B and S6). Thus, we anticipated that activation with either 365 or 405 nm LEDs would be possible.

The uncaging efficiency for ***o*NB-MDPP** was determined using ^{31}P NMR spectroscopy (Figure 1C and section S3.2). Release of **MDPP** upon 405 nm LED irradiation (100 mW/cm^2) was tracked by proxy of methyldiphenylphosphine oxide (**MDPPO**) generated in situ. A concentrated solution of ***o*NB-MDPP** (72 mM), together with PPh_3 as an internal standard (36 mM) ensured approximately quantitative light absorption and strong NMR signals at low conversions (<10%). This minimized the competitive absorption of the ***o*NB** byproduct to determine the internal uncaging quantum yield (Φ_u). The **MDPPO** signal appeared at irradiation times of 2.5, 5, and 10 min, revealing a respectable Φ_u of 5.5 ± 0.3%, which was in line with our prior findings for dimethoxy ***o*NB** photocages.[34,35]

Real-time Fourier transform infrared (RT-FTIR) spectroscopy in an attenuated total reflectance (ATR) configuration was employed to characterize thiol−isocyanate addition to PTUs activated by onium photocages (Figure 2A). A model resin comprising hexamethylene diisocyanate (HMDI) and pentaerythritol tetrakis(3-mercaptopropionate) (PETMP) with a 1:1 functional group ratio was tested with four ***o*NB**−onium photocages (0.5 mol %), which were readily miscible without the need for solvent. Irradiation with a violet LED (405 nm, 20 mW/cm^2) caused rapid polymerization without inhibition after the 10 s dark period (Figure 2B). Monomer to polymer conversion (ρ) was determined by monitoring the disappearance of the isocyanate (N═C═O) stretch at ∼2270 cm^{-1}.[36] The three phosphonium photocages resulted in comparable polymerization rates (∼170−190 mM/s), which were >2 times higher than the ammonium photocage (∼70 mM/s). Notably, photopolymerization only occurred with [BPh_4]$^-$ counterions and not Br^-, [BF_4]$^-$, and [B(Ph-(CF$_3$)$_2$)$_4$]$^-$ ([BAr^F_4]$^-$) (Figures S13−S15), signifying the importance of counterion selection. We hypothesized that ***o*NB** undergoes photocyclization and elimination[37] to release an ammonium− or phosphonium−borate ion pair followed by its degradation in an analogous fashion to that described for [BPh_4]$^-$ guanidinium salts irradiated with deep-UV light (≤254 nm),[16] which yields arylborane fragments and the corresponding amine or phosphine (Figure S20).

Given similar photopolymerization rates for the different phosphonium photocages, we selected ***o*NB-MDPP** for future studies due to its qualitatively enhanced resin miscibility. Exposing the same model resin to intensities ranging from 2 to 80 mW/cm^2 resulted in an ∼16-fold increase in polymerization rate, from 35 to 574 mM/s (based on isocyanate conversion), respectively (Figure 2C). This provided an approximately linear relationship between polymerization rate and light intensity (Figure S19), characteristic of base-catalyzed thiol-Michael addition reactions which lack bimolecular termination pathways.[38] Notably, ∼50% monomer conversion occurs within 10 s of irradiation for intensities ≥20 mW/cm^2, and the maximum conversion of ∼60% was thought to result from vitrification.

Using an intensity of 20 mW/cm^2, temporal control was assessed by extending the initial dark period from 10 to 300 s during RT-FTIR experiments (Figure 2D). Furthermore, the phosphonium photocages were directly compared with previously reported ionic xanthone carboxylate, neutral ***o*NB**, and coumarinylmethyl photocages bearing various guanidine

https://doi.org/10.1021/jacs.4c07220
J. Am. Chem. Soc. 2024, 146, 19704−19709

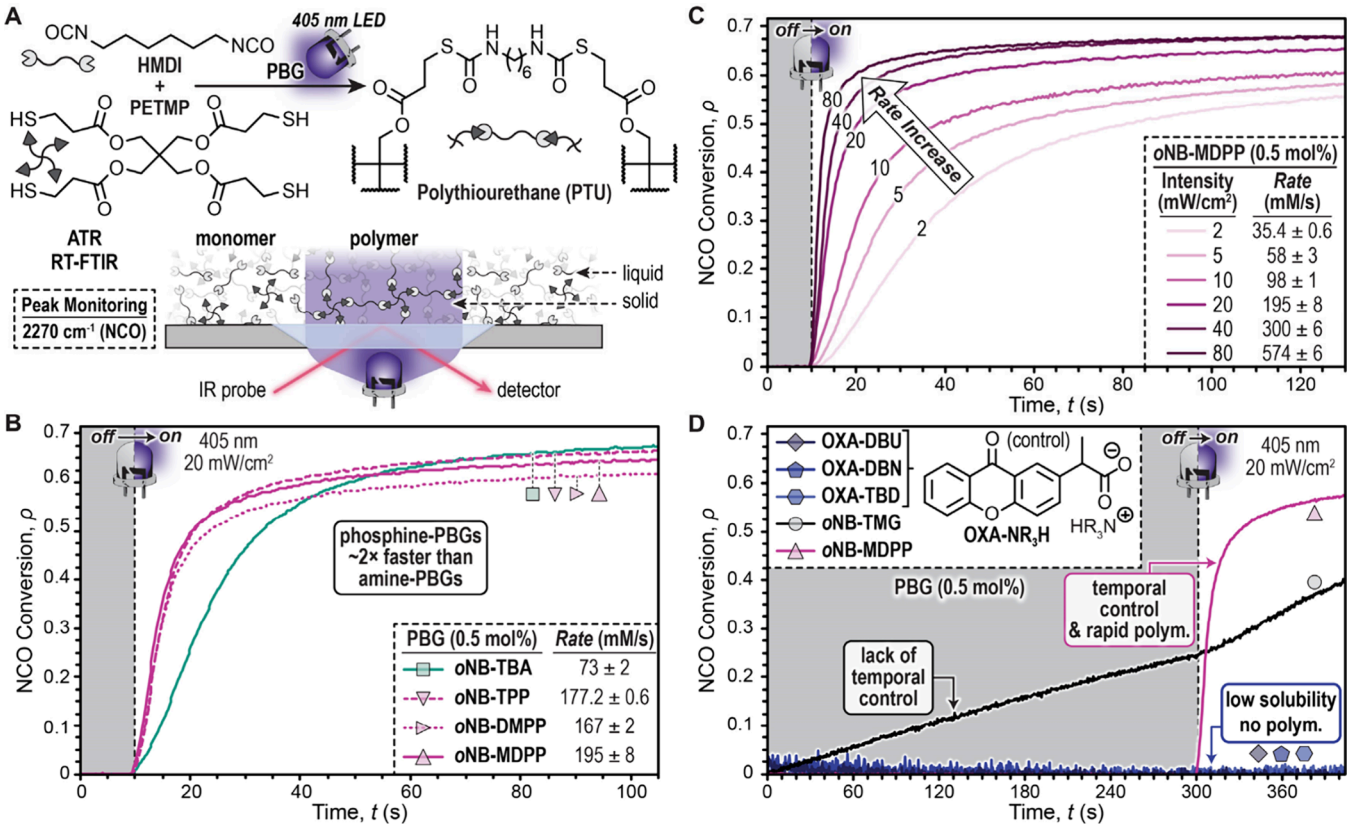

Figure 2. Thiol–isocyanate photopolymerizations monitored using RT-FTIR spectroscopy. (A) Chemical structures for model resin components and illustration of the ATR RT-FTIR setup used to monitor isocyanate (NCO) conversion (ρ) over time (t) in forming PTUs. HMDI and PETMP were used in a 2:1 molar ratio with no added solvent. (B) Representative photopolymerizations with ***o*NB** photocages exposed to violet light (405 nm, 20 mW/cm^2) after a 10 s dark period. (C) Influence of LED intensity on photopolymerization using ***o*NB-MDPP**. (D) Temporal control of ***o*NB-MDPP** against a guanidine-caged xanthone carboxylate salt and neutral TMG photocages. The LED was turned on at 300 s (405 nm, 20 mW/cm^2).

cargoes (Figures 2D and S16–S18). The xanthone salts had poor miscibility in the resin, which coupled with their weak violet-light absorption, resulted in no observable polymerization. However, adding solvent CH_3CN (9 wt %) to aid miscibility led to rapid gelation. Similarly, neutral photocages containing TMG led to PTU formation in the dark, precluding their utility in photocurable resins requiring temporal control (e.g., 3D printing). We hypothesized that the caged TMG-carbamates activated isocyanates to nucleophilic attack by thiols. In stark contrast, the present phosphonium photocages caused no dark reaction yet underwent rapid polymerization upon light exposure.

To showcase the breadth of properties achievable with PTU 3D printing, two disparate resins were created using inexpensive commercial isocyanates and thiols: a hard, strong resin and a soft, extensible one (Figure 3A). The hard PTU resin comprised isophorone diisocyanate (IPDI) and trimethylolpropane tris(3-mercaptopropionate) (TMPMP) with an ethoxylated analog (ETTMP-700) in an ∼9:1 molar ratio. Qualitatively, TMPMP provided stronger, less brittle materials relative to PETMP, with further mechanical property improvements observed by adding ETTMP-700 (see sections S3.5 and S3.8 for more details). The soft resin comprised *p*-tolylene 2,4-diisocyanate-terminated poly(propylene glycol) (TDI-PPG) together with 2,2′-(ethylenedioxy)diethanethiol (DODT) and TMPMP in an ∼13:1 molar ratio.

Photopolymerizations with a 405 nm LED (80 mW/cm^2) were monitored using RT-FTIR spectroscopy in a transmission configuration, with 100 μm thick samples to match printing (Figure 3B). In both the hard and soft resins, 10 wt % acetonitrile was added to improve resin stability and photocage mixing, where photocage crystallinity notably influenced the ease of solubilization (Figure S26). With 1 and 2 mol % ***o*NB-MDPP** in the hard and soft resins, respectively, rapid photopolymerizations ensued. Specifically, isocyanate conversion rates of 1280 and 375 mM/s for the hard and soft resins were measured, reaching a conversion plateau in ∼30 s. According to the Carothers equation (section S3.5), the hard and soft formulations should theoretically reach their respective gel points at 83% and 98% conversion, which correspond to ∼13 and ∼15 s by RT-FTIR spectroscopy, respectively. Photorheology of the soft resin under identical conditions (405 nm LED, 80 mW/cm^2, 100 μm thickness) provided a gel point of ∼7 s (Figure S27). In either case, this displayed the high monomer conversions necessary for gelation to occur in networks formed via a step-growth mechanism, which contrasts with standard acrylic resins used for 3D printing, where uncontrolled radical chain growth causes gelation at low conversions.[39] Delayed gelation and the formation of more uniform networks have the potential to improve stability and mechanical performance by reducing the density of residual reactive functionality and topological defects.

https://doi.org/10.1021/jacs.4c07220
J. Am. Chem. Soc. 2024, 146, 19704–19709

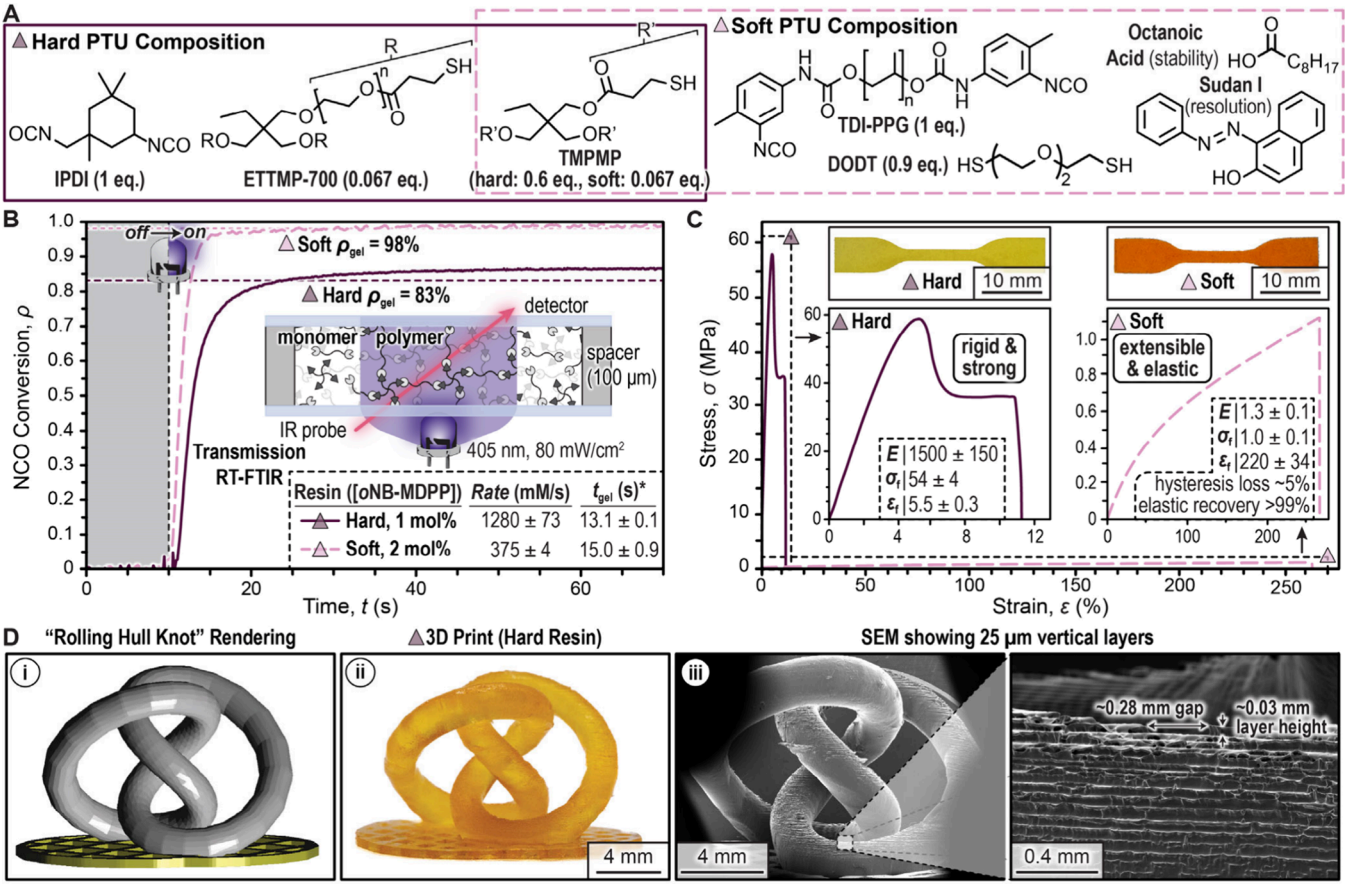

Figure 3. Onium photocages in PTU 3D printing. (A) Chemical structures for hard and soft resin formulations, which include 9 wt % CH_3CN. (B) Photopolymerization kinetics monitored using transmission RT-FTIR. (C) Uniaxial tensile testing data of hard and soft dogbones prepared using DLP 3D printing with violet light (405 nm, 80 mW/cm^2) at exposure times of 20 and 15 s/100 μm layer, respectively. The insets show photographs of the hard and soft dogbones along with zoomed-in stress−strain plots. (D) Complex 3D print with (i) digital rendering, (ii) photograph of hard knot (printed at 8 s/25 μm layer), and (iii) SEM images.

Tensile testing of DLP 3D-printed dogbones using exposure times of 20 and 15 s/100 μm layer (405 nm LED, 80 mW/cm^2) for the hard and soft resins, respectively, was accomplished next (Figure 3C and section S3.9). The hard system provided materials with a strength (maximum stress, σ_{max}) of 54 MPa and stiffness (Young's modulus, E) of ∼1500 MPa. In contrast, the soft system provided materials with E ∼ 1 MPa that could stretch (fracture strain, ε_f) to ∼200% of their original size with hysteresis (<5%) and elastic recovery (>99%) comparable to natural rubber (Figures S31−S35). These extreme properties are competitive with optimized industrial acrylic resins.[40,41]

As a final demonstration, complex 3D objects were produced with both resin systems (Figure 3D and sections S3.10 and S3.11). A rolling hull knot was selected as a challenging 3D structure that necessitated high lateral and vertical resolution along with sufficient mechanical integrity to withstand the printing process (Figures 3D and S36−S45). For the hard and soft resins, exposure times of 8 and 3.5 s/25 μm layer, respectively, were used. Notably, the soft resin was more reactive because of the use of aryl isocyanates in place of aliphatic ones, leading to a slow background reaction over the course of hours after mixing (Figures S46−S49). A small amount of octanoic acid (0.15 mol %) was added to the soft resin as a stabilizer, along with Sudan I (0.0003 mol %) as an opaquing agent to improve resolution. The prints were characterized with scanning electron microscopy, revealing excellent print fidelity, with layer thicknesses averaging 36 ± 7 and 98 ± 6 μm for 25 and 100 μm hard knots, respectively. Additionally, lateral features as small as ∼100 μm were possible based on resolution prints from the hard and soft resins (Figures S28−S30).

In summary, phosphonium ***o*NB** photocages were synthesized with a scalable three-step process and used to catalyze the rapid formation of PTUs upon exposure to violet (405 nm) light. High uncaging yields (Φ_u = 5.5%) of **MDPP** led to thiol−isocyanate polyaddition reactions with maximum conversions reached in <30 s. Finally, ***o*NB-MDPP** was used in DLP 3D printing to produce high-resolution structures with disparate mechanical properties, from strong and stiff to soft and elastic. We postulate that coupling various ***o*NB** derivatives, or possibly other triplet-forming dyes, with onium $[BPh_4]^-$ salts may serve as a platform to temporally generate organobases with light. This would enable light-driven advanced manufacturing of materials beyond the traditionally employed acrylics and epoxies such as those with improved long-term stability and unique mechanical properties, recyclability, stimuli-responsive behavior, and multifunctionality.

https://doi.org/10.1021/jacs.4c07220
J. Am. Chem. Soc. 2024, 146, 19704−19709

■ ASSOCIATED CONTENT

Supporting Information

The Supporting Information is available free of charge at https://pubs.acs.org/doi/10.1021/jacs.4c07220.

Additional experimental (materials, instrumentation, and synthesis) and characterization details (PDF)

Accession Codes

CCDC 2358565 contains the supplementary crystallographic data for this paper. These data can be obtained free of charge via www.ccdc.cam.ac.uk/data_request/cif, or by emailing data_request@ccdc.cam.ac.uk, or by contacting The Cambridge Crystallographic Data Centre, 12 Union Road, Cambridge CB2 1EZ, U.K.; fax: +44 1223 336033.

■ AUTHOR INFORMATION

Corresponding Author

Zachariah A. Page − *Department of Chemistry, The University of Texas at Austin, Austin, Texas 78712, United States;* orcid.org/0000-0002-1013-5422; Email: zpage@utexas.edu

Authors

Meghan T. Kiker − *Department of Chemistry, The University of Texas at Austin, Austin, Texas 78712, United States;* orcid.org/0000-0003-0620-2079

Ain Uddin − *Department of Chemistry, The University of Texas at Austin, Austin, Texas 78712, United States*

Lynn M. Stevens − *Department of Chemistry, The University of Texas at Austin, Austin, Texas 78712, United States;* orcid.org/0000-0002-7956-8277

Connor J. O'Dea − *Department of Chemistry, The University of Texas at Austin, Austin, Texas 78712, United States*

Keldy S. Mason − *Department of Chemistry, The University of Texas at Austin, Austin, Texas 78712, United States;* orcid.org/0000-0003-2481-4570

Complete contact information is available at: https://pubs.acs.org/10.1021/jacs.4c07220

Author Contributions

‡M.T.K. and A.U. contributed equally.

Notes

The authors declare the following competing financial interest(s): U.S. Provisional Patent Application No. 63/563,072 (Onium Salts as Photocages and Methods of Using the Same) was filed March 8, 2024.

■ ACKNOWLEDGMENTS

The authors acknowledge primary support from the National Science Foundation under Grant MSN-2107877 (A.U., M.T.K., L.M.S., C.J.O., Z.A.P.). Partial support was provided by the Robert A. Welch Foundation under Grant F-2007 (A.U., Z.A.P.) and the Research Corporation for Science Advancement via Cottrell Scholars Award 28184 (Z.A.P.). The authors thank Dr. Hashini Munasinghe in Dr. Michael Aubrey's laboratory for support with PXRD analysis and Dr. Serhii Vasylevskyi in the X-ray Core Facility of UT Austin for his determination of the single-crystal X-ray structure of *o*NB-MDPP.

■ ABBREVIATIONS

LED, light-emitting diode; PTU, polythiourethane; *o*NB, *o*-nitrobenzyl; PBG, photobase generator; TBA, tributylamine; TPP, tripropylphosphine; DMPP, dimethylphenylphosphine; MDPP, methyldiphenylphosphine; MDPPO, methyldiphenylphosphine oxide; $[BPh_4]^-$, tetraphenylborate; $[BF_4]^-$, tetrafluoroborate; $[B(Ph(CF_3)_2)_4]^-$ ($[BAr^F{}_4]^-$), tetrakis[3,5-bis(trifluoromethyl)phenyl]borate; OXA-DBU, 2-(9-oxoxanthen-2-yl)propionic acid 1,8-diazabicyclo[5.4.0]undec-7-ene salt; OXA-DBN, 2-(9-oxoxanthen-2-yl)propionic acid 1,5-diazabicyclo[4.3.0]non-5-ene salt; OXA-TBD, 2-(9-oxoxanthen-2-yl)propionic acid 1,5,7-triazabicyclo[4.4.0]dec-5-ene salt; RT-FTIR, real-time Fourier transform infrared; ATR, attenuated total reflectance; QY, quantum yield; HOMO, highest occupied molecular orbital; LUMO, lowest unoccupied molecular orbital; DLP, digital light processing; HMDI, hexamethylene diisocyanate; PETMP, pentaerythritol tetrakis(3-mercaptopropionate); TMG, tetramethylguanidine; IPDI, isophorone diisocyanate; TDI-PPG, tolylene 2,4-diisocyanate-terminated poly(propylene glycol) (average $M_n \sim 2300$); ETTMP, ethoxylated trimethylolpropane tris(3-mercaptopropionate); DODT, 3,6-dioxa-1,8-octanedithiol; TMPMP, trimethylolpropane tris(3-mercaptopropionate); SEM, scanning electron microscopy

■ REFERENCES

(1) Dumur, F. The Future of Visible Light Photoinitiators of Polymerization for Photocrosslinking Applications. *Eur. Polym. J.* **2023**, *187*, No. 111883.

(2) Bao, Y.; Paunović, N.; Leroux, J. C. Challenges and Opportunities in 3D Printing of Biodegradable Medical Devices by Emerging Photopolymerization Techniques. *Adv. Funct. Mater.* **2022**, *32* (15), No. 2109864.

(3) Bagheri, A.; Jin, J. Photopolymerization in 3D Printing. *ACS Appl. Polym. Mater.* **2019**, *1* (4), 593−611.

(4) Jung, K.; Corrigan, N.; Ciftci, M.; Xu, J.; Seo, S. E.; Hawker, C. J.; Boyer, C. Designing with Light: Advanced 2D, 3D, and 4D Materials. *Adv. Mater.* **2020**, *32*, No. 1903850.

(5) Lee, Y.; Boyer, C.; Kwon, M. S. Visible-Light-Driven Polymerization towards the Green Synthesis of Plastics. *Nat. Rev. Mater.* **2022**, *7* (2), 74−75.

(6) Mandsberg, N. K.; Aslan, F.; Dong, Z.; Levkin, P. A. 3D Printing of Reactive Macroporous Polymers via Thiol−Ene Chemistry and Polymerization-Induced Phase Separation. *Chem. Commun.* **2024**, *60* (45), 5872−5875.

(7) Kirillova, A.; Yeazel, T. R.; Gall, K.; Becker, M. L. Thiol-Based Three-Dimensional Printing of Fully Degradable Poly(Propylene Fumarate) Star Polymers. *ACS Appl. Mater. Interfaces* **2022**, *14* (34), 38436−38447.

(8) Pal, S.; Asha, S. K. Thiol-Ene-Based Degradable 3D Printed Network from Bio Resource Derived Monomers Ethyl-Lactate and Isosorbide. *Eur. Polym. J.* **2024**, *205*, No. 112761.

(9) Thijssen, Q.; Quaak, A.; Toombs, J.; De Vlieghere, E.; Parmentier, L.; Taylor, H.; Van Vlierberghe, S. Volumetric Printing of Thiol-Ene Photo-Cross-Linkable Poly(ε-Caprolactone): A Tunable Material Platform Serving Biomedical Applications. *Adv. Mater.* **2023**, *35* (19), No. 2210136.

(10) Zhang, X.; Xi, W.; Gao, G.; Wang, X.; Stansbury, J. W.; Bowman, C. N. O-Nitrobenzyl-Based Photobase Generators: Efficient Photoinitiators for Visible-Light Induced Thiol-Michael Addition Photopolymerization. *ACS Macro Lett.* **2018**, *7* (7), 852−857.

(11) Long, K. F.; Wang, H.; Dimos, T. T.; Bowman, C. N. Effects of Thiol Substitution on the Kinetics and Efficiency of Thiol-Michael Reactions and Polymerizations. *Macromolecules* **2021**, *54* (7), 3093−3100.

(12) Zhang, X.; Xi, W.; Wang, C.; Podgórski, M.; Bowman, C. N. Visible-Light-Initiated Thiol-Michael Addition Polymerizations with Coumarin-Based Photobase Generators: Another Photoclick Reaction Strategy. *ACS Macro Lett.* **2016**, *5* (2), 229−233.
(13) Zhang, X.; Wang, X.; Chatani, S.; Bowman, C. N. Phosphonium Tetraphenylborate: A Photocatalyst for Visible-Light-Induced, Nucleophile-Initiated Thiol-Michael Addition Photopolymerization. *ACS Macro Lett.* **2021**, *10* (1), 84−89.
(14) Li, Z.; Shen, W.; Liu, X.; Liu, R. Efficient Unimolecular Photoinitiators for Simultaneous Hybrid Thiol-Yne-Epoxy Photopolymerization under Visible LED Light Irradiation. *Polym. Chem.* **2017**, *8* (9), 1579−1588.
(15) Yu, X.; Chen, J.; Yang, J.; Zeng, Z.; Chen, Y. Synthesis and Photoinitiation Properties of a Novel Quaternary Ammonium Tetraphenylborate Salt. *J. Appl. Polym. Sci.* **2006**, *100* (1), 399−405.
(16) Sun, X.; Gao, J. P.; Wang, Z. Y. Bicyclic Guanidinium Tetraphenylborate: A Photobase Generator and a Photocatalyst for Living Anionic Ring-Opening Polymerization and Cross-Linking of Polymeric Materials Containing Ester and Hydroxy Groups. *J. Am. Chem. Soc.* **2008**, *130* (26), 8130−8131.
(17) Placet, E.; Pinaud, J.; Gimello, O.; Lacroix-Desmazes, P. UV-Initiated Ring Opening Polymerization of l -Lactide Using a Photobase Generator. *ACS Macro Lett.* **2018**, *7* (6), 688−692.
(18) Stukenkemper, T.; Jansen, J. F. G. A.; Lavilla, C.; Dias, A. A.; Brougham, D. F.; Heise, A. Polypeptides by Light: Photo-Polymerization of: *N*-Carboxyanhydrides (NCA). *Polym. Chem.* **2017**, *8* (5), 828−832.
(19) Goodrich, S. L.; Hill, M. R.; Olson, R. A.; Sumerlin, B. S. Photo-Liberated Amines for *N*-Carboxyanhydride (PLANCA) Ring-Opening Polymerization. *Polym. Chem.* **2021**, *12* (28), 4104−4110.
(20) Zivic, N.; Sadaba, N.; Almandoz, N.; Ruipérez, F.; Mecerreyes, D.; Sardon, H. Thioxanthone-Based Photobase Generators for the Synthesis of Polyurethanes via the Photopolymerization of Polyols and Polyisocyanates. *Macromolecules* **2020**, *53* (6), 2069−2076.
(21) Perrot, D.; Croutxé-Barghorn, C.; Allonas, X. UV-Curable Thio-Ether-Urethane Network with Tunable Properties. *J. Polym. Sci., Part A: Polym. Chem.* **2016**, *54* (19), 3119−3126.
(22) Matsushima, H.; Shin, J.; Bowman, C. N.; Hoyle, C. E. Thiol-Isocyanate-Acrylate Ternary Networks by Selective Thiol-Click Chemistry. *J. Polym. Sci., Part A: Polym. Chem.* **2010**, *48*, 3255−3264.
(23) Zivic, N.; Kuroishi, P. K.; Dumur, F.; Gigmes, D.; Dove, A. P.; Sardon, H. Recent Advances and Challenges in the Design of Organic Photoacid and Photobase Generators for Polymerizations. *Angew. Chem., Int. Ed.* **2019**, *58* (31), 10410−10422.
(24) Lai, H.; Zhang, J.; Xing, F.; Xiao, P. Recent Advances in Light-Regulated Non-Radical Polymerisations. *Chem. Soc. Rev.* **2020**, *49* (6), 1867−1886.
(25) Lu, P.; Ahn, D.; Yunis, R.; Delafresnaye, L.; Corrigan, N.; Boyer, C.; Barner-Kowollik, C.; Page, Z. A. Wavelength-Selective Light-Matter Interactions in Polymer Science. *Matter* **2021**, *4* (7), 2172−2229.
(26) Guy, N.; Giani, O.; Blanquer, S.; Pinaud, J.; Robin, J. J. Photoinduced Ring-Opening Polymerizations. *Prog. Org. Coat.* **2021**, *153*, No. 106159.
(27) Tong, J.; Mao, Y.; Pi, J.; Luo, J.; Liu, R. Exploiting Dynamic Thiourethane Covalent Bonds for Enhanced Adhesion of UV-Curable Metal Coatings. *Prog. Org. Coat.* **2023**, *177*, No. 107438.
(28) Yue, H.; Zhou, J.; Huang, M.; Hao, C.; Hao, R.; Dong, C.; He, S.; Liu, H.; Liu, W.; Zhu, C. Recyclable, Reconfigurable, Thermadapt Shape Memory Polythiourethane Networks with Multiple Dynamic Bonds for Recycling of Carbon Fiber-Reinforced Composites. *Polymer* **2021**, *237*, No. 124358.
(29) Zhou, J.; Yue, H.; Huang, M.; Hao, C.; He, S.; Liu, H.; Liu, W.; Zhu, C.; Dong, X.; Wang, D. Arbitrarily Reconfigurable and Thermadapt Reversible Two-Way Shape Memory Poly(Thiourethane) Accomplished by Multiple Dynamic Covalent Bonds. *ACS Appl. Mater. Interfaces* **2021**, *13* (36), 43426−43437.
(30) Qian, Y.; Dong, F.; Guo, L.; Lu, S.; Xu, X.; Liu, H. Self-Healing and Reprocessable Terpene Polysiloxane-Based Poly(thiourethane-urethane) Material with Reversible Thiourethane Bonds. *Biomacromolecules* **2023**, *24* (3), 1184−1193.
(31) Fan, C. J.; Wen, Z. B.; Xu, Z. Y.; Xiao, Y.; Wu, D.; Yang, K. K.; Wang, Y. Z. Adaptable Strategy to Fabricate Self-Healable and Reprocessable Poly(Thiourethane-Urethane) Elastomers via Reversible Thiol-Isocyanate Click Chemistry. *Macromolecules* **2020**, *53* (11), 4284−4293.
(32) Lopez de Pariza, X.; Varela, O.; Catt, S. O.; Long, T. E.; Blasco, E.; Sardon, H. Recyclable Photoresins for Light-Mediated Additive Manufacturing towards Loop 3D Printing. *Nat. Commun.* **2023**, *14* (1), 5504.
(33) Sarker, A. M.; Kaneko, Y.; Nikolaitchik, A. V.; Neckers, D. C. Photoinduced Electron-Transfer Reactions: Highly Efficient Cleavage of C-N Bonds and Photogeneration of Tertiary Amines. *J. Phys. Chem. A* **1998**, *102* (28), 5375−5382.
(34) Kiker, M. T.; Uddin, A.; Stevens, L. M.; Chung, K.-Y.; Lu, P.; Page, Z. A. Visible Light Activated Coumarin Photocages: An Interplay between Radical and Organobase Generation to Govern Thiol−Ene Polymerizations. *Polym. Chem.* **2023**, *14* (33), 3843−3850.
(35) Chung, K.-Y.; Uddin, A.; Page, Z. A. Record Release of Tetramethylguanidine Using a Green Light Activated Photocage for Rapid Synthesis of Soft Materials. *Chem. Sci.* **2023**, *14* (39), 10736−10743.
(36) Radice, S.; Turri, S.; Scicchitano, M. Fourier Transform Infrared Studies on Deblocking and Crosslinking Mechanisms of Some Fluorine Containing Monocomponent Polyurethanes. *Appl. Spectrosc., AS* **2004**, *58* (5), 535−542.
(37) Bley, F.; Schaper, K.; Görner, H. Photoprocesses of Molecules with 2-Nitrobenzyl Protecting Groups and Caged Organic Acids. *Photochem. Photobiol.* **2008**, *84* (1), 162−171.
(38) Claudino, M.; Zhang, X.; Alim, M. D.; Podgórski, M.; Bowman, C. N. Mechanistic Kinetic Modeling of Thiol−Michael Addition Photopolymerizations via Photocaged "Superbase" Generators: An Analytical Approach. *Macromolecules* **2016**, *49* (21), 8061−8074.
(39) Ahn, D.; Stevens, L. M.; Zhou, K.; Page, Z. A. Rapid High-Resolution Visible Light 3D Printing. *ACS Cent. Sci.* **2020**, *6* (9), 1555−1563.
(40) Bomar. *3D Printing*. https://bomar-chem.com/markets/3d-printing (accessed 2024-04-27).
(41) Carbon. *3D Printing Materials for Real-World Applications*. https://www.carbon3d.com/materials (accessed 2024-04-27).

https://doi.org/10.1021/jacs.4c07220
J. Am. Chem. Soc. 2024, 146, 19704−19709